

ATMOSPHERIC RIVERS AND LARGE AVALANCHE EVENTS IN SLIDE CANYON, UTAH, USA

Matthew C. Primomo\*

Utah Department of Transportation, Salt Lake City, Utah, USA

**ABSTRACT:** An atmospheric river (AR) is a narrow and long atmospheric structure that is responsible for the majority of horizontal water vapor transport outside of the tropics (Zhu and Newell 1998). A way of assessing AR's and strong moisture transport events in general is through the presence of high values of integrated water vapor transport (IVT), which provides a quantitative measure of how much water is being transported in the atmosphere.

Slide Canyon is a large avalanche path in Provo Canyon, Utah. High IVT ( $>180\text{Kg/m/s}$ ) were observed during the 3-day period preceding all of the D4 avalanche events in Slide Canyon since 1978. Arrivals of ARs are fairly infrequent here, but when they do heavy, and prolonged precipitation may occur. The majority of storm total precipitation occurs during the warm phase of the storm (pre-frontal). Large avalanches tend to occur early on during these events. A case study of the four most recent occurrences with further analyses are included.

**KEYWORDS:** (atmospheric river, integrated vapor transport, large avalanche, orographic, precipitation).



Fig 1: Slide Canyon as seen from the Southeast on an average winter.

---

\* *Corresponding author address:*  
Matthew C. Primomo 1748 South 200 East Salt  
Lake City, UT 84115 tel: 970-485-0659 email:  
mprimomo@utah.gov

## 1. INTRODUCTION

Integrated vapor transport (IVT) is a quantitative measure of how much water is being transported in the atmosphere. It is calculated by taking the product of wind speed and vapor throughout a column of air. An atmospheric river (AR) is a narrow

and lengthy atmospheric structure that is responsible for the majority of horizontal water vapor transport outside of the tropics (Zhu and Newell 1998). They originate in the tropics and/or via local moisture convergence (Bao et al. 2006), and form narrow bands which stretch poleward (Zhu and Newell 1998). When these features make landfall, heavy and prolonged precipitation events can occur. Once an AR makes landfall, the presence of orography can enhance the ascent of air parcels and result in highly variable precipitation rates during an event. ARs contribute significantly to flooding and snowpack changes in western North America (Neiman et al. 2008).

The strongest events are often accompanied by anomalously warm temperatures, rain-on-snow, flooding, landslides, and debris flows (Neiman et al. 2008). ARs were present in all of the seven floods on the Russian River in California between 1997 and 2006 (Ralph et al. 2006). Heavy rains during an AR caused the Nisqually River to overtake a National Park Service Road in Mount Rainier National Park in November 2006 (Neiman et al 2008). An example of a likely AR coincidence with a historic avalanche cycle is the winter storm in the Central Chilean Andes during early August 2015 (see TAR 34.2) in which Colin Mitchell reports 169cm of snow with 211mm of snow water equivalent in 52 hours (Mitchell 2016) and a historic avalanche cycle.

The structure of an atmospheric river typically involves a deep layer of a prefrontal moisture plume oriented parallel to the cold front of a mid-latitude cyclone (Zhu and Newell 1998). Ralph et al (2004) found that often AR's produce a Low Level Jet (LLJ) during the pre-frontal phase (warm phase) of the storm, which is then followed by deep convection as part of the cold front (cold phase) and often shallower layer of moisture after frontal passage. Ralph (2006) found that AR's were present in all of the storms that produced floods on the Russian River in California, and LLJ's appeared in waves during the heavy precipitation during those storms.

Mountain ranges enhance lift, dry air masses out, and inhibit the downstream spread of more moisture (Hughes and Mahoney 2014, Rutz et al. 2015). AR's that begin over the Pacific most often cause precipitation along the Sierra Nevada and Cascade Ranges, but occasionally reach further inland. A number of different patterns are responsible for AR penetration into the Northwest, and Southwest interior (Rutz and Steenburgh 2014). When they pass through lowland corridors from

the west, they are able to survive a longer distance and thus are more likely to be affected by a mountain range (Rutz and Steenburgh 2014). Birkeland and Mock (2001) found that avalanche extremes at four different sites in the West occur when moisture is allowed to flow through low elevation pathways to the site. Each of the four sites they studied has its own unique pathway for a storm track in order to achieve optimal precipitation influence.

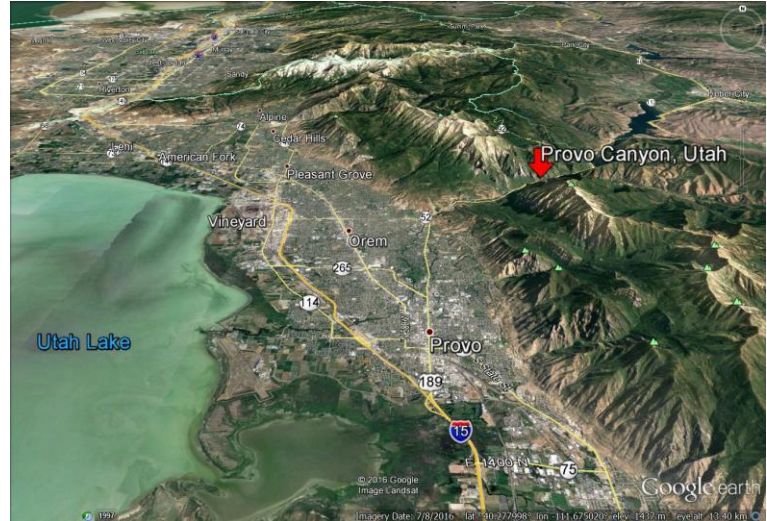


Fig 2. Google Earth image of Provo Canyon, Utah, USA

One optimal pathway that has become recognizable because it favors Provo Canyon is via the Southern Cascades in Oregon and Northern California. Provo Canyon is a major weakness in a chain of the Southern Wasatch Mountains that rise 2,130m vertical off the valley floor (see Fig. 2). The spine of these mountains has a Northwest to Southeast orientation. Strong orographic enhancement of precipitation is often observed during events with West to Southwest winds. Slide Canyon is a large avalanche path in Provo Canyon characterized by long planar slopes (See Figure 1). The avalanche starting zones face Northeast to Southeast with an upper ridgetop elevation of 3244m. The track is a long channel with a consistent pitch, and the runout is an alluvial fan where US-189 passes through Provo Canyon at 1594m. The Mid Mountain Weather Station located at Sundance Mountain Resort is the closest, most representative site for snowfall and precipitation data. It sits at 2270m and roughly one mile to the Northeast from the center of the main starting zone, one drainage removed.

In early February of 2014 a potent Atmospheric River made landfall into the area. It was characterized by strong West-Northwest upper level jet stream winds, strong Southwest lower level winds, high water vapor content, and strong warm air advection. There was a one-hour period with 9.4mm recorded with the ETI sensor at the Mid Mountain site. Temperatures slowly rose while precipitation rates continued to exceed 2.5mm/hr for some time. Widespread instabilities developed and a large natural avalanche cycle began. Many large avalanche paths on the Timpanogos and Cascade massifs ran full track. These paths are 1100m to 1600m vertical drop and produce avalanches of D4+ in size. The initial failure was suspected to have been caused by lower density stellar crystals, however a ~30cm thick layer of 2mm basal facets that were on average 4-Finger hard were also overloaded on many slopes. We ended up with more than double the storm totals as nearby sites, and overachieved all weather forecasts.

## 2. METHODS

Jonathan Rutz has been maintaining a catalog of IVT ([http://www.inscc.utah.edu/~rutz/ar\\_catalogs/](http://www.inscc.utah.edu/~rutz/ar_catalogs/)) and the presence of ARs by identifying whether a moisture plume is >2000km long and has IVT>250Kg/m/s throughout (Rutz et al. 2014). The data used is in a 2.5 degree resolution (roughly 277km<sup>2</sup>), so the area where Provo Canyon lies is quite large, and IVT values are likely smoothed over due to the complex topography. IVT forecasts have been recently made available at the Center for Western Weather and Water Extremes (CW3E:woodland.ucsd.edu/?cat=12).

Archived Special Sensor Microwave Imager (SSM/I/S) images are used to verify the large scale pattern and origin of the moisture. These can be found at [www.esrl.noaa.gov/psd/psd2/coastal/satres/archive.html](http://www.esrl.noaa.gov/psd/psd2/coastal/satres/archive.html). The images show the concentration of IVT over the oceans of the world.

14 avalanche occurrences were found in the data set that came within 100m of, or covered US-189. 100m is used because that seems to be a threshold of avalanches within the data set; many lower magnitude avalanches were recorded that stopped much further than 100m, the few that made it that close were the 14 used. The next closest running avalanche was recorded to have come 428m from the road. This was triggered by a heli-bombing mission with special mention of an ice crust being involved in the snowpack at the time. The 14 avalanches ran either naturally, with heli-bombing, or with artillery. They were both hard and soft slabs,

but debris likely always showed signs of wet flowing motion. These all classify as at least D4 in size, two were D4.5. The largest was in 1978 when debris was reported to be 9m to 28m deep along a 275m length of road. It took nearly three days of continuous work for highway crews to clear the road (Daily Herald 1978).

Four events are then analyzed further. These are the four most recent events of D4 size, and also the four in which quality precipitation and wind data are available for.

## 3. RESULTS

To get an idea of average IVT during any given time in the winter, the 6 hour periods were averaged during the timeframe of November 1 through April 30. Average IVT during this time for the winter of 2010/11 through winter of 2014/15 was 69.5 Kg/m/s.

Table 1 shows maximum IVT values for three days prior to avalanche occurrences from Slide Canyon, where debris made it <100m from US-189. Eight of the 14 occurrences met the requirements for an AR (>250 Kg/m/s) within three days period prior. 12 of 14 occurrences had an IVT that exceeded 220 Kg/m/s within the three days preceding an avalanche. The lowest maximum IVT value before an avalanche was 182 Kg/m/s.

Tbl. 1: IVT (Kg/m/s) and Avalanche Occurrences.  
\* Signifies event qualifies as an AR

<i>Avalanche Occurrence Date</i>	<i>Max IVT within 24 Hrs of Occurrence</i>	<i>Max IVT 24- 48 Hrs of Occurrence</i>	<i>Max IVT 48- 72 Hrs of Occurrence</i>
19780303	113.6	172.2	182.3
19860213*	270.5	87.4	65
19860224	194.1	154.3	82.2
19940221*	88.3	30.3	317.4
19960128	223.4	204	68.8
19960201	104.3	230.7	241.2
19970126*	256.9	321.5	70.1
19970127*	123.7	321.5	201.2
20041208*	339.6	283.2	150.7
20050109	228.7	230.4	205.8
20101219*	359.6	179.6	19.9
20101229*	264.4	46.2	60.3
20140208*	254.4	230.2	128.8
20151221	155.3	221.6	97
Average	212.6	193.8	135.0

Table 2 details four events that caused large avalanches in Slide Canyon. Event 1 is believed to have been a D4 like the rest, but exact details on time of occurrence and size are not well documented. A major avalanche cycle in the area is well documented, however. Events 1, 2, and 3 ran naturally, event 4 was triggered by artillery. Figures 6, 7, 8, and 9 (Section 7) show what the events looked like with the SSMI/S imagery roughly 12 hours prior to an avalanche occurrence. Long plumes of water vapor are observed over the Pacific Ocean and push inland over the western US, consistent with the mesoscale structure of an AR. The major findings from the data summary from these four storms are;

- Heavy precipitation rates and periods of prolonged precipitation are often accompanied by high values of IVT.
- Maximum precipitation rates reached 9.5mm to 11.5mm an hour.
- Precipitation rates sometimes reached their max during cold air passage.
- Prolonged, and heavy precipitation fell during the warm phase of the storm.
- The majority of the storm total precipitation fell during the warm phase of the storm.
- All four of the avalanches studied occurred early on, during the warm phase of the storm.
- Temperature at the Mid Mountain site during time of avalanche is between -2C and -3C.

Tbl 2: Storm event summary of the last four D4 avalanches from Slide Canyon

Event Number	1	2	3	4
Storm Start	12/16/2010	12/28/2010	2/7/2014	2/20/2015
Storm End	12/21/2010	1/1/2011	2/11/2014	12/24/2015
Total Time (Hours)	122	90	111	113
HSTW (mm)	249.9	146.8	167.4	184.9
HST (Change in HS) (cm)	109	69	79	135
Max Precip Rate (mm/Hr)	11.4	10.4	9.4	9.9
Max Precip Rate during warm phase (mm/Hr)	9.4	10.4	9.4	9.9
Hours with = or > 2.54mm/hr during warm phase	35	16	28	27
Total Precip during warm phase (mm)	211.6	88.1	160.3	154.7
Max Precip Rate during cold phase (mm/Hr)	11.4	10.2	2.5	4.6
Hours with = or > 2.54mm/hr during cold phase	5	5	2	3
Total Precip during cold phase (mm)	38.1	58.7	7.1	30.2
Avy during warm or cold phase?	Warm	Warm	Warm	Warm
Precip to Avy (mm)	NA	45.7	74.7	88.1
Change in HS to Avy (cm)	NA	30.1	41.4	52.8
Temp at time of Avy (C)	NA	-2.8	-1.9	-2.9
Max IVT 24 Hour	361.8	264.4	254.5	155.3
Max IVT 48 Hour	270.4	46.2	230.2	221.6
Max IVT 72 Hour	147.2	60.3	128.8	97.0
Classifies as AR?	Yes	Yes	Yes	No

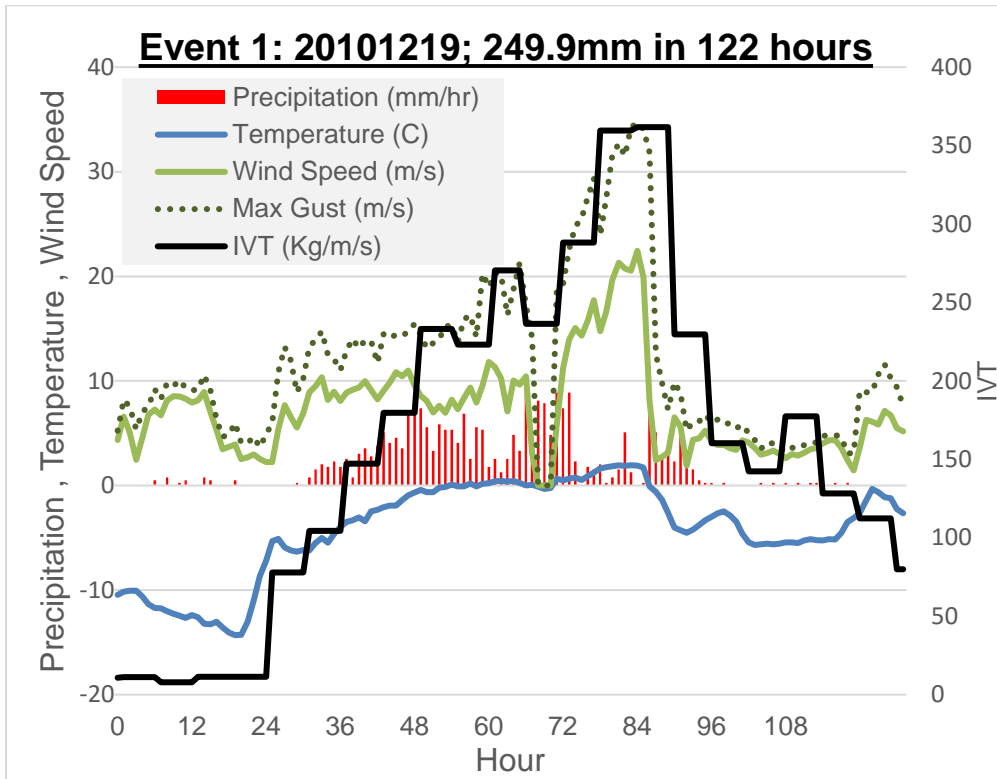


Fig. 3: Event 1 details. Avalanche is believed to have occurred near hour 65.

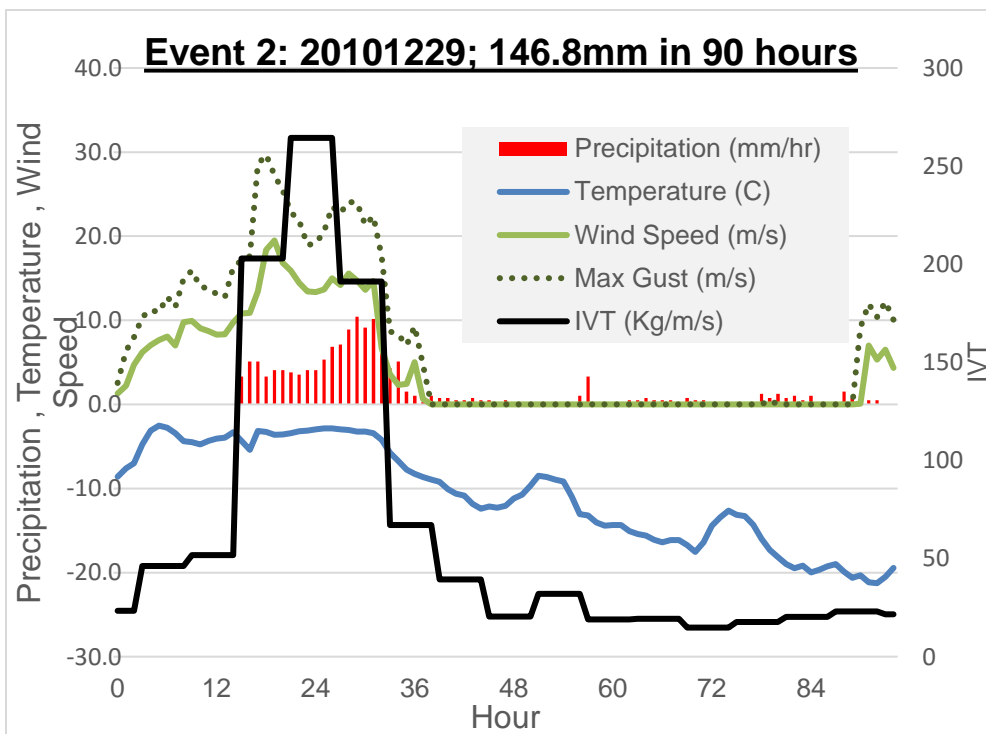


Fig. 4: Event 2 details. Avalanche occurred at hour 26.

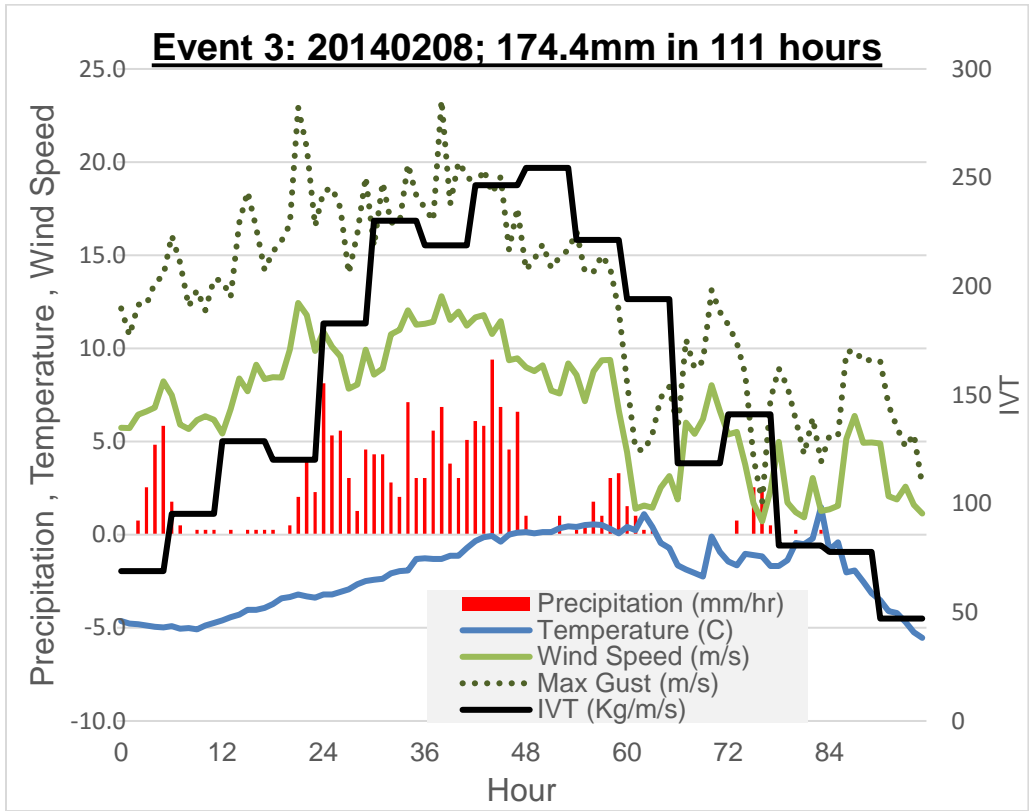


Fig. 5: Event 3 details. Avalanche occurred at hour 34.

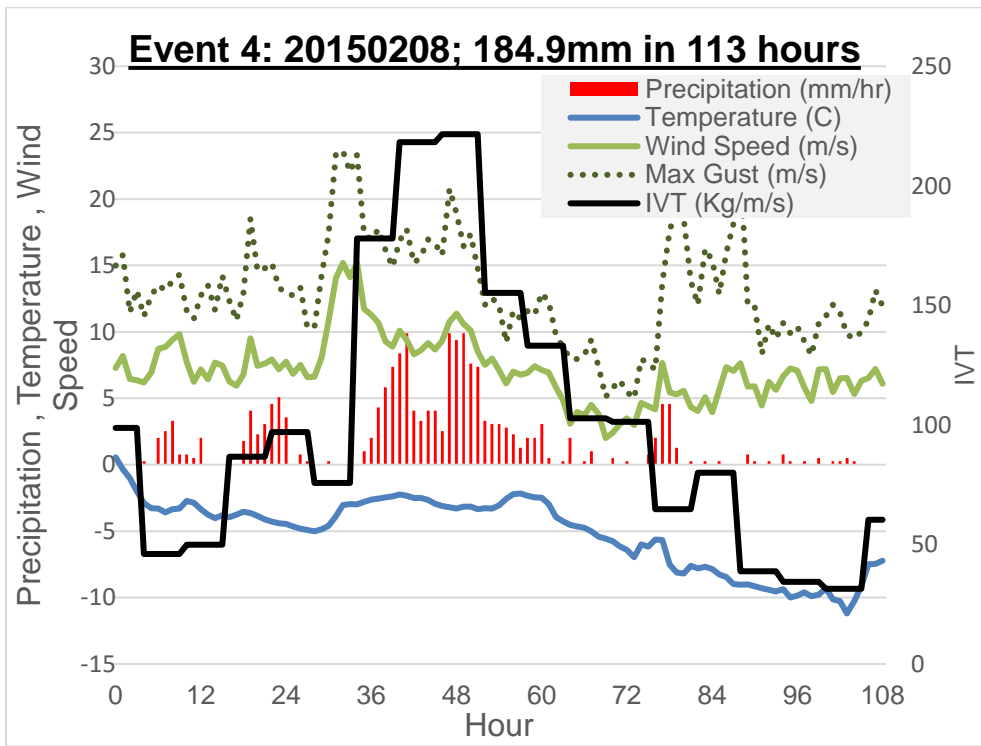


Fig. 6: Event 4 details: Avalanche occurred at hour 46.

#### 4. DISCUSSION

Atmospheric rivers and periods of high Integrated Vapor Transport in general are an important factor when it comes to large avalanches in Slide Canyon. Prolonged and heavy precipitation contributes to D4 avalanches, and heavy and prolonged precipitation often occurs as part of the warm phase, or pre frontal phase of an atmospheric river. Large avalanches tend to occur early on with these storms, so awareness of the presence of an AR structure as part of an incoming storm is an invaluable tool to help decision making processes while forecasting for Provo Canyon.

The particular orientation and track of each storm is what may or may not allow it to reach the Canyon, and AR events are fairly uncommon in this area. However, it is likely that if a mountain range has a low elevation pathway from the coast then AR's play a role in heavy wintertime precipitation episodes. Further research could focus on identification of the orientation and track of AR's that reached a particular area, and a discriminate analyses of which types tend to produce the heaviest precipitation for individual sites.

#### 5. REFERENCES

Bao J-W., S. A. Michelson, P. J. Neiman, F. M. Ralph, and J. M. Wilczak, 2006: Interpretation of Enhanced Integrated Water Vapor Bands Associated with Extratropical Cyclones: Their Formation and Connection to Tropical Moisture. *Monthly Weather Review*, **134**, 1063–1080.

Birkeland Karl W., Mock, C., and Shinker, J.J., 2001. Avalanche Extremes and Atmospheric Circulation Patterns. *Annals of Glaciology*, **32**, 135-140.

Data, NCAR/NCEP reanalysis courtesy Jonathan Rutz: [http://www.inscc.utah.edu/~rutz/ar\\_catalogs/ncep\\_2.5/](http://www.inscc.utah.edu/~rutz/ar_catalogs/ncep_2.5/)

Data, UDOT Avalanche Office, Provo Canyon: [mpri-momo@utah.gov](mailto:mpri-momo@utah.gov)

Hughes Miami, Kelly M. Mahoney, Paul J. Neiman, Benjamin J. Moore, Michael Alexander, and F. Martin Ralph, 2014: The Landfall and Inland Penetration of a Flood-Producing Atmospheric River in Arizona. Part II: Sensitivity of Modeled Precipitation to Terrain Height and Atmospheric River Orientation. *J. Hydrometeorol*, **15**, 1954–1974.

Kirby Matthew, Zimmerman, Patterson, and Rivera, 2012. A 9170-year record of decadal-to-multi-centennial scale pluvial episodes from the coastal Southwest United States: a role for atmospheric rivers? *Quaternary Science Reviews* **46**, 57-65.

Leung, L. R., and Y. Qian, 2009. Atmospheric Rivers Induced Heavy Precipitation and Flooding in the Western U.S. Simulated by the WRF Regional Climate Model, *Geophysical Research Letters*, **36**, L03820.

McClung David and Peter Schaerer, 2006. *The Avalanche Handbook, Edition 3: The Mountaineers Books.*  
Mitchell, Colin. Personal Communication 2/25/2016.

Neiman Paul J., et al, 2008: Diagnosis of an Intense Atmospheric River Impacting the Pacific Northwest: Storm Summary and Offshore Vertical Structure Observed with COSMIC Satellite Retrievals. *Monthly Weather Review*, **136**, 4398–4420.

Newell Reginald E., et al, 1992. Tropospheric Rivers?-A Pilot Study. *Geophysical Research Letters*, **12**, 24, 2401-2404.  
Ron I. Perla, 1970. On Contributory Factors in Avalanche Hazard Evaluation. *Canadian Geotechnical Journal*, **7**, 414-419.

Ralph Martin F., Paul J. Neiman, Gary A. Wick, Seth I. Gutman, Michael D. Dettinger, Daniel R. Cayan, and Allen B. White, 2006. Flooding on California's Russian River: Role of Atmospheric Rivers. *Geophysical Research Letters*, **33**, L13801.

Ralph Martin F., et al., 2004. Satellite and CALJET Aircraft Observations of Atmospheric Rivers over the Eastern North Pacific Ocean during the Winter of 1997/98. *Monthly Weather Review*, **132**, 1721–1745.

Rutz Jonathan J., W. James Steenburgh, and F. Martin Ralph, 2015. The Inland Penetration of Atmospheric Rivers over Western North America: A Lagrangian Analysis. *Monthly Weather Review*, **143**, 1924–1944.

Rutz Jonathan J., and Steenburgh J., 2014. Climatological Characteristics of Atmospheric Rivers and Their Inland Penetration over the Western US. *American Meteorological Society*, **142**, 905-921.

Gao, Y., J. Lu, L. R. Leung, Q. Yang, S. Hagos, and Y. Qian, 2015. Dynamical and Thermodynamical Modulations on Future Changes of Landfalling Atmospheric Rivers Over Western North America, *Geophysical Research Letters*, **42**, 7179–7186.

Zhu Yong and Newell, R, 1998. A Proposed Algorithm for Moisture Fluxes From Atmospheric Rivers. *American Meteorological Society*, **126**, 725-735.

#### 6. ADDITIONAL INFORMATION

##### CONFLICT OF INTEREST

The creation of this document was not supported financially or materially by the ISSW. None of the authors benefit financially from the production or sale of ISSW proceedings nor have they received any related grants or patents.

##### ACKNOWLEDGEMENTS

I would like to acknowledge Chris Covington, William Nalli, Jonathan Rutz PhD, and Benjamin Hatchett MSc for their guidance and support.

#### 7. FIGURES 6, 7, 8, AND 9

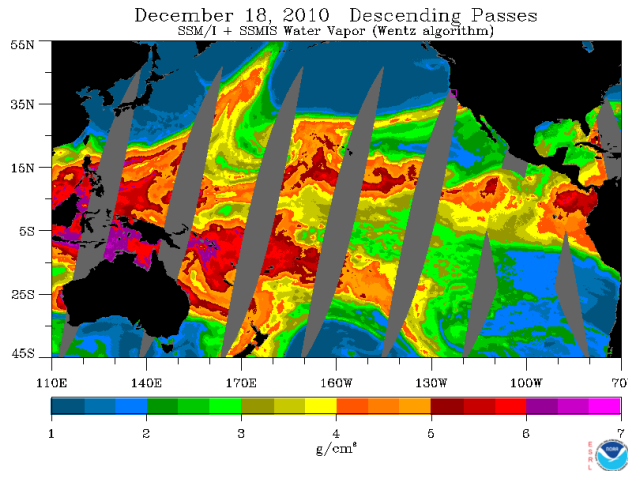


Fig. 6: SSMI/S Image roughly 12 hours prior to Event 1 (20101219).

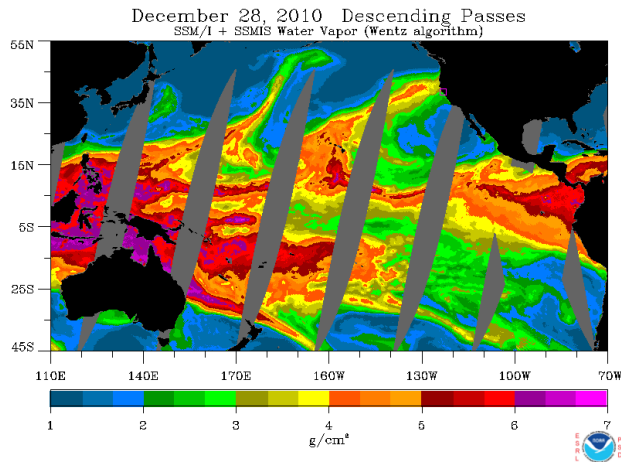


Fig. 7: SSMI/S Image roughly 12 hours prior to Event 2 (20101229).

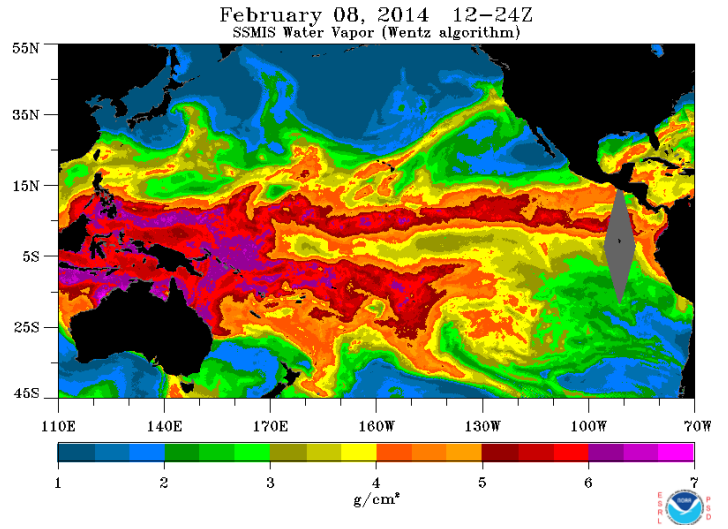


Fig. 8: SSMI/S Image roughly 12 hours prior to Event 3 (20140208).

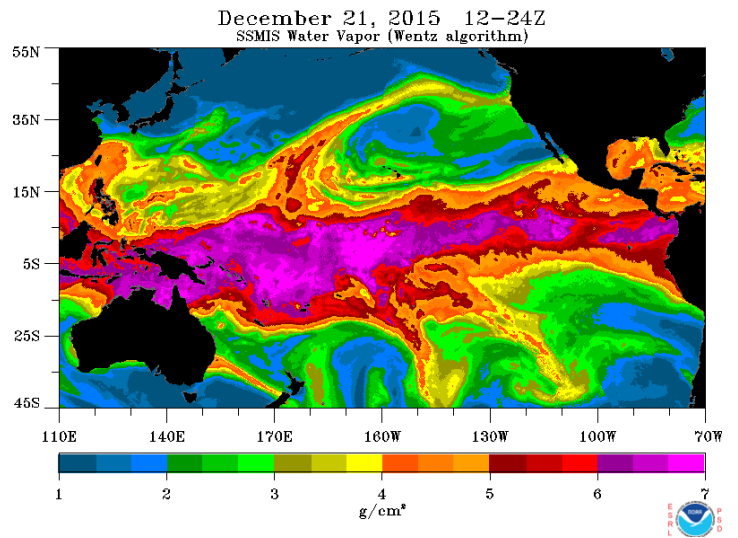


Fig. 9: SSMI/S Image roughly 12 hours prior to Event 4 (20151222).